JACS
JOURNAL OF THE AMERICAN CHEMICAL SOCIETY
Article
pubs.acs.org/JACS

Gold(III) Mediated Activation and Transformation of Methane on Au_1-Doped Vanadium Oxide Cluster Cations $AuV_2O_6^+$

Zi-Yu Li,[†] Hai-Fang Li,[†,‡] Yan-Xia Zhao,*[,†] and Sheng-Gui He*[,†]

[†]Beijing National Laboratory for Molecular Sciences, State Key Laboratory for Structural Chemistry of Unstable and Stable Species, Institute of Chemistry, Chinese Academy of Sciences, Beijing 100190, People's Republic of China

[‡]University of Chinese Academy of Sciences, Beijing 100049, People's Republic of China

Supporting Information

ABSTRACT: Gold in the +III oxidation state (Au^{III}) has been proposed as a promising species to mediate challenging chemical reactions. However, it is difficult to characterize the chemistry of individual Au^{III} species in condensed-phase systems mainly due to the interference from the Au^{I} counterpart. Herein, by doping Au atoms into gas-phase vanadium oxide clusters, we demonstrate that the Au^{III} cation in the $AuV_2O_6^+$ cluster is active for activation and transformation of methane, the most stable alkane molecule, into formaldehyde under mild conditions. In contrast, the $AuV_2O_6^+$ cluster isomers with the Au^{I} cation can only absorb CH_4. The clusters were generated by laser ablation and mass selected to react with CH_4, CD_4, or CH_2D_2 in an ion trap reactor. The reactivity was characterized by mass spectrometry and quantum chemistry calculations. The structures of the reactant and product ions were identified by using collision-induced and 425 nm photo-induced dissociation techniques.

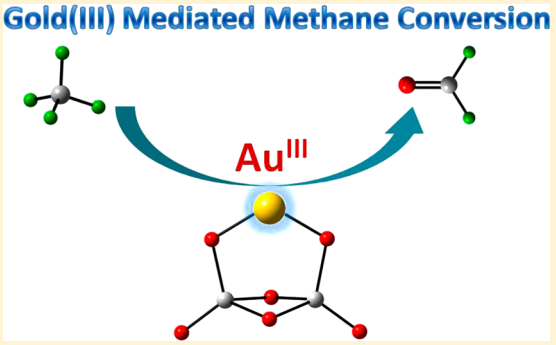

1. INTRODUCTION

Gold catalysts have shown remarkable performance in many important processes including CO oxidation, hydrogenation, and C−H activation.[1] Extensive research efforts have been devoted to elucidating the molecular origin of gold catalysis.[2,3] It is emphasized that the oxidation state of gold is a key factor governing the catalytic activity.[3] The cationic gold in the +III oxidation state (Au^{III}) has a high standard reduction potential and strong Lewis acid property[4] and is not only regarded as the active species in oxidation of CO and hydrogenation of alkenes,[5] but also proposed to provide new opportunities in challenging reactions,[6] such as transformation of methane, the "holy grail" in chemistry.[7] However, the understanding and development of the Au^{III} chemistry are limited due to the difficulties in characterizing the chemical bonding and reactivity of individual Au^{III} species in condensed-phase systems. For instance, Periana and co-workers reported a way of catalyzing methane to methanol using cationic gold (Au^{I} and Au^{III}) in strong acid solvents, while the question of whether one or both Au^{I} and Au^{III} species are active for the C−H activation of methane remains unclear.[8] It is desirable to adopt an alternative approach to investigate the chemistry of individual cationic gold species.

Studying individual active species confined on atomic clusters[9,10] that can be explored under isolated, controlled, and reproducible conditions has been recently demonstrated to be successful. The spin and charge effects on the reactivity of atomic oxygen radical anions ($O^{\bullet-}$) on atomic clusters have been revealed.[10,11] The extraordinary activity of single noble metal atoms including Au_1 and Pt_1 on metal oxide clusters could also be discovered.[12,13] The investigations of the Au_1-doped metal oxide clusters have demonstrated that the conversions of Au^{I}−O into Au^{-I}−M (M = Ti, Fe, Nb, Ce, and Al) species could drive CO oxidation, dihydrogen activation, and so on.[12] However, possibly because Au^{III} has a high standard reduction potential,[4] the preparation of Au^{III} onto metal oxide clusters was unsuccessful in the previous experiments[12,14] and the chemical bonding and reactivity of the important Au^{III} species on metal oxide clusters have been unknown yet.

Inspired by the experimental evidence that the interaction of Au with vanadia results in the formation of Au^{III} species,[15] Au_1-doped vanadium oxide clusters $AuV_xO_y^+$ were prepared and reacted with methane in an ion trap reactor under mild conditions. Among many of the prepared Au_1-doped vanadium oxide clusters, the $AuV_2O_6^+$ cluster was highly reactive and showed the capability to transform methane. In conjunction with the structure characterizations and density functional calculations, the methane transformation can be attributed to the Au^{III} species in $AuV_2O_6^+$. It is noteworthy that the structures[16] and reactivity[17] of (undoped) vanadium oxide clusters have been extensively studied previously.

Received: December 13, 2015
Revised: April 17, 2016
Published: July 6, 2016

DOI: 10.1021/jacs.6b03940
J. Am. Chem. Soc. 2016, 138, 9437−9443

2. METHODS

Experimental Method. The $AuV_xO_y^+$ clusters were generated by laser ablation of a mixed metal disk compressed with Au and V powders (molar ratio: Au/V = 1/1) in the presence of 0.5% O_2 seeded in a He carrier gas with the backing pressure of 6.5 standard atmospheres. The cluster ions of interest were mass-selected by a quadrupole mass filter (QMF). To well resolve $AuV_2O_6^+$ (m/z = 385 for ^{16}O) from Au_2^+ (m/z = 384) and increase the ion-transmittance of the QMF, $^{18}O_2$ was used as the oxygen source to generate the clusters. The mass-selected cluster ions entered into a linear ion trap (LIT) reactor where they were confined and cooled by collisions with a pulse of He gas for 0.9 ms and then interacted with a pulse of CH_4, CD_4, or CH_2D_2 for around 1.2 ms. The instantaneous gas pressure of He in the reactor is around 6−8 Pa (~3000 collisions) and longer cooling time (>0.9 ms) did not affect the reaction efficiency,[13a,18] indicating that the $AuV_2O_6^+$ ions had been thermalized before they reacted with methane. The partial pressures of the reactant molecules ranged from about 1 mPa to more than 20 mPa depending on the reaction systems. The temperature of the cooling gas (He), the reactant gases (CH_4, CD_4, and CH_2D_2), and the LIT reactor is around 298 K. The cluster ions ejected from the LIT were detected by a reflectron time-of-flight mass spectrometer (TOF-MS). The details to run the TOF-MS,[19] the QMF,[20] and the LIT[18] can be found in our previous works.

The collision-induced dissociation (CID) experiments were performed for structural investigations by introducing argon into the LIT for collisions with $AuV_2O_6^+$ ions of which the translational energies could be fixed at different values. The time period for collision of $AuV_2O_6^+$ with Ar in the trap was short (<20 μs) and the pressure of Ar in the ion trap was low (≤30 mPa). The average number of collisions[21] between $AuV_2O_6^+$ and Ar was estimated to be 0.05, indicating that multiple collisions were improbable. The daughter and the parent ions were detected by the TOF-MS.

A tandem TOF-MS coupled with an OPO (optical parametric oscillator, Continuum, Horizon I) laser was employed to study the photo-induced dissociation (PID)[22] of mass-selected cluster ions. Briefly, the reactant and product ions in the reaction of $AuV_2O_6^+$ with CH_4 passed through two identical reflectors with Z-shaped configuration in the primary TOF-MS. The ions of interest were mass selected by a mass gate and then interacted with the OPO laser beam (425 nm). The daughter (fragment) and the parent ions passed through the reflector of the secondary TOF-MS and then were detected by a dual microchannel plate detector.

Theoretical Method. The density functional theory (DFT) calculations using Gaussian 09 program[23] were carried out to investigate the structures of $AuV_2O_6^+$ as well as the reaction mechanisms with CH_4. The TZVP basis sets[24] for C, H, O, and V atoms and the D95V basis sets combined with the Stuttgart/Dresden relativistic effective core potentials (denoted as SDD in Gaussian software)[25] for Au atom were adopted. The TPSS functional[26] performed very well for the bond energies of Au−O, Au−V, Au−C, Au−H, V−O, C−H, and O−H (see Supporting Information),[27] so the TPSS results were given throughout this work. A Fortran code based on genetic algorithm[28] was used to generate the initial guess structures of $AuV_2O_6^+$. The reaction mechanism calculations involved geometry optimization of reaction intermediates (IMs) and transition states (TSs) through which the IMs transfer to each other. The initial guess structures of the TS species were obtained through relaxed potential energy surface scans using a single or multiple internal coordinates.[29] Vibrational frequency calculations were performed to check that each of the IMs and TSs has zero and only one imaginary frequency, respectively. Intrinsic reaction coordinate calculations were performed so that a TS connects two appropriate local minima. To determine reliable energies of the low-lying isomers of $AuV_2O_6^+$ clusters, single-point energy calculations with high-level quantum chemistry method of RCCSD(T)[30] were performed at the DFT optimized geometries. The zero-point vibration corrected energies (ΔH_0) in unit of eV are reported in this work.

The Rice−Ramsperger−Kassel−Marcus theory[31] (RRKM) and RRKM-based variational transition state theory[32] (VTST) were used to calculate the rate constants of traversing transition states from intermediates and for CH_4 desorption from adsorption complexes. For these calculations, the energy of the initially formed reaction intermediate (E) and the energy barrier ($E^{\ddagger}$) for each step were needed. The reaction intermediate possesses the vibrational energies (E_{vib}) of $AuV_2O_6^+$ and CH_4, the center of mass kinetic energy (E_k), and the binding energy (E_b) between $AuV_2O_6^+$ and CH_4. The values of E_{vib} and E_b were taken from the DFT calculations and $E_k = \mu v^2/2$, in which μ is the reduced mass and v is the velocity (≈ 1000 m/s). The VTST calculations involved geometry optimizations of $AuV_2O_6CH_4^+$ by fixing the distance between the $AuV_2O_6^+$ and CH_4 moieties at various values. The densities and the numbers of states required for RRKM and VTST calculations were obtained by the direct count method[33] with the DFT-calculated vibrational frequencies under the approximation of harmonic vibrations.

3. RESULTS AND DISCUSSION

Cluster Reactivity. The TOF mass spectra for the interactions of laser ablation generated, mass-selected, and thermalized $AuV_2O_6^+$ cluster cations with CH_4, CD_4, or CH_2D_2 are shown in Figure 1. Upon interaction with 2 mPa CH_4 in the reactor for about 1.2 ms, in addition to the molecular association product $AuV_2O_6CH_4^+$, additional products assigned as $AuV_2O_5H_2^+$, $V_2O_6CH_3^+$, $V_2O_5H^+$, and $V_2O_5H_2^+$ were generated (Figure 1b). The relative intensities of these products increase as the CH_4 pressure increases (Figure 1c), which suggests reactions 1−4 below:

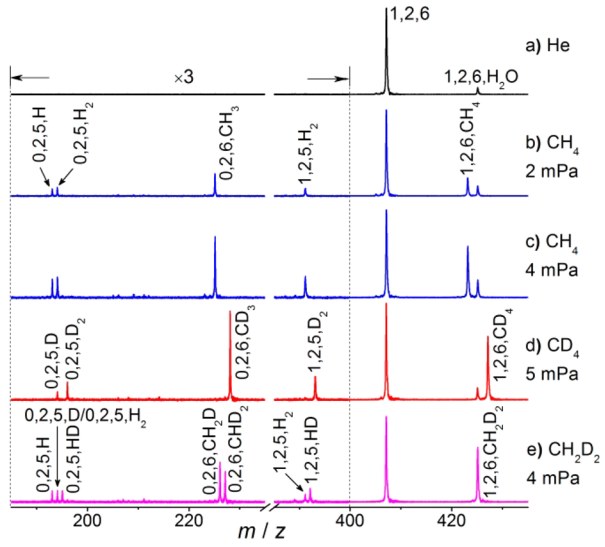

Figure 1. TOF mass spectra for the reactions of $AuV_2{}^{18}O_6^+$ (a) with 2 mPa CH_4 (b), 4 mPa CH_4 (c), 5 mPa CD_4 (d), and 4 mPa CH_2D_2 (e) for 1.2 ms. The relative signal magnitudes are amplified by a factor of 3 for m/z < 400. The $Au_xV_yO_z^+$ and $Au_xV_yO_zX^+$ are labeled as x,y,z and x,y,z,X, respectively. The weak $AuV_2O_6H_2O^+$ in (a) is due to the reaction of $AuV_2O_6^+$ with residual water from the gas handling system.

$$AuV_2O_6^+ + CH_4 \rightarrow V_2O_6CH_3^+ + AuH \quad 53\% \qquad (1)$$

$$AuV_2O_6^+ + CH_4 \rightarrow AuV_2O_5H_2^+ + CH_2O \quad 18\% \qquad (2)$$

$$AuV_2O_6^+ + CH_4 \rightarrow V_2O_5H^+ + AuOCH_3(CH_2O + AuH)\ 13\% \qquad (3)$$

$$AuV_2O_6^+ + CH_4 \rightarrow V_2O_5H_2^+ + AuOCH_2(CH_2O + Au)\ 16\% \qquad (4)$$

DOI: 10.1021/jacs.6b03940
J. Am. Chem. Soc. 2016, 138, 9437−9443

The isotopic labeling experiments with CD_4 (Figure 1d) and CH_2D_2 (Figure 1e) confirmed the above reaction channels.

The experimentally generated atomic clusters can have different structural isomers with different reactivity, which can be characterized with the reactant-gas-pressure (P) dependent experiments (Figure 2 and Figure S4 in the Supporting Information). It turns out that with respect to the increase of P, the relative ion signal of $AuV_2O_6^+$ (I_R) follows a double-exponential decay:

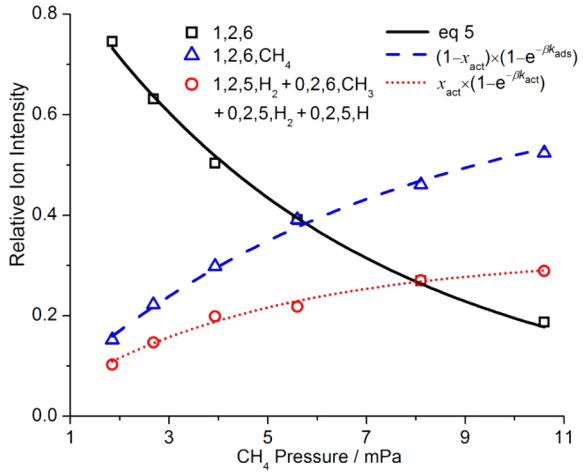

Figure 2. Variations of relative ion intensities with respect to the CH_4 pressure in the reaction of $AuV_2O_6^+$ with CH_4.

$$I_R = x_{act} \times \exp(-\beta k_{act}) + (1 - x_{act}) \times \exp(-\beta k_{ads}) \quad (5)$$

in which $\beta = \frac{P}{k_B T} t_R$, k_B is the Boltzmann constant, T is the temperature (~298 K), t_R is the reaction time (~1.2 ms), x_{act} and $1 - x_{act}$ are the normalized abundances of the $AuV_2O_6^+$ isomers that lead to methane transformation (reactions 1–4) and methane adsorption (formation of $AuV_2O_6CH_4^+$), respectively.

The least-squares-fitted pseudo-first-order rate constants k_{act} and k_{ads} along with the values of x_{act} are listed in Table 1. It indicates that (34 ± 3) % of the experimentally generated $AuV_2O_6^+$ resulted in reactions 1–4, while the left component (66 ± 3) % only adsorbed methane. The transformation channels have small kinetic isotopic effects: $k_{act}(CH_4)/k_{act}(CD_4)$ = 1.4 ± 0.2 and $k_{act}(CH_4)/k_{act}(CH_2D_2)$ = 1.2 ± 0.1. The small kinetic isotopic effect is likely due to the reactions occurring nearly at the collision rate. The theoretical collision rate constant (k_{coll})[21] between $AuV_2O_6^+$ and CH_4 is 9.8×10^{-10} cm^3 molecule^{-1} s^{-1}, so the reaction efficiency (k_{act}/k_{coll}) amounts to 80% for the reactive isomer of $AuV_2O_6^+$ with CH_4. It is noteworthy that the adsorption rate constants k_{ads} are almost identical for three different reactant gases CH_4, CD_4, and CH_2D_2, indicating the nondissociative methane adsorption on the clusters.

Table 1. Relative Abundance of the Reactive Cluster Isomer and the Rate Constants (k_{act} and k_{ads} in 10^{-10} cm^3 molecule^{-1} s^{-1}) for Methane Transformation and Adsorption in the Reactions of $AuV_2O_6^+$ with CH_4, CD_4, and CH_2D_2

molecules	$x_{act} \times 100\%$	k_{act}	k_{ads}
CH_4	(32 ± 1)	7.8 ± 0.7	5.0 ± 0.2
CD_4	(35 ± 2)	5.4 ± 0.6	5.1 ± 0.3
CH_2D_2	(36 ± 1)	6.4 ± 0.4	5.1 ± 0.2

Structural Characterization. The structures of the reactant cluster ions $AuV_2O_6^+$ and the association product ions $AuV_2O_6CH_4^+$ were characterized with the CID and PID experiments, respectively, and the results are shown in Figure 3.

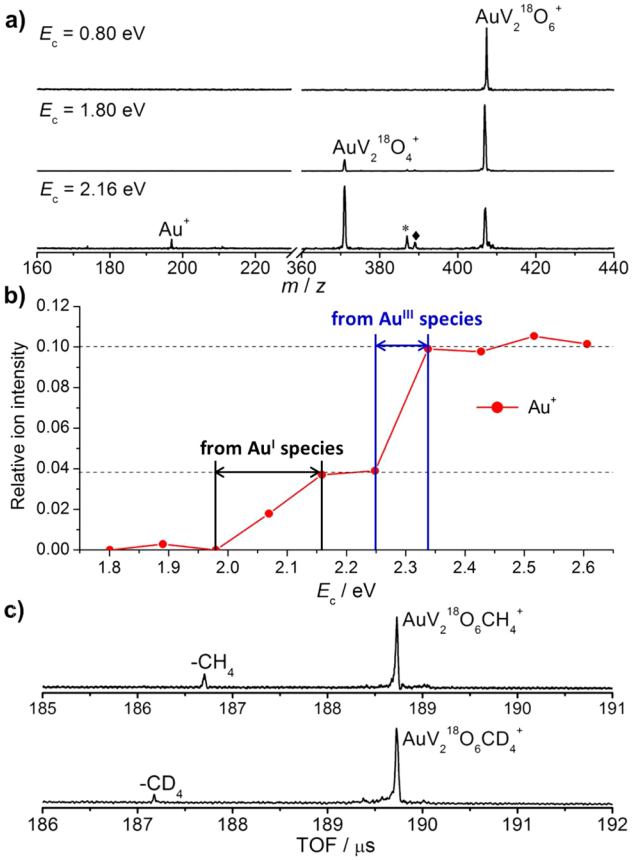

Figure 3. (a) CID spectra of $AuV_2{}^{18}O_6^+$ with 30 mPa Ar. Center-of-mass collisional energy (E_c) is given. Peaks marked as "*" and "◆" are due to water impurities. (b) The relative ion intensity of Au^+ with respect to E_c. (c) PID spectra of $AuV_2{}^{18}O_6CH_4^+$ and $AuV_2{}^{18}O_6CD_4^+$ at 425 nm.

When the mass-selected $AuV_2O_6^+$ cations collided with Ar in the ion trap, the resulting mass spectra were crucially dependent on the center-of-mass collisional energies (E_c). At E_c < 1.98 eV, the only product ions formed ($AuV_2O_4^+$) corresponded to the loss of O_2. Upon increasing E_c, a signal for Au^+, with concomitant elimination of V_2O_6, appeared (Figure 3a). The CID experiments indicate that molecular oxygen species (O_2^{2-} or O_2^-) would be presented in $AuV_2O_6^+$, and the binding energy of the O–O unit is lower than that of Au^+ in $AuV_2O_6^+$. Furthermore, two growth regions (1.98–2.16 eV and 2.25–2.34 eV in Figure 3b) for the Au^+ signal were observed, suggesting the presence of $AuV_2O_6^+$ isomers with different Au^+ binding energies.

In the PID experiments, when the 425 nm laser beam interacted with the association complexes $AuV_2O_6CH_4^+$, the daughter ion peak assigned as $AuV_2O_6^+$ was observed (Figure 3c): $AuV_2O_6CH_4^+ + h\nu \rightarrow AuV_2O_6^+ + CH_4$, which was also confirmed by the isotopic labeling experiment. The PID results strongly suggest that CH_4 is nondissociatively adsorbed in $AuV_2O_6CH_4^+$.

DOI: 10.1021/jacs.6b03940
J. Am. Chem. Soc. 2016, 138, 9437–9443

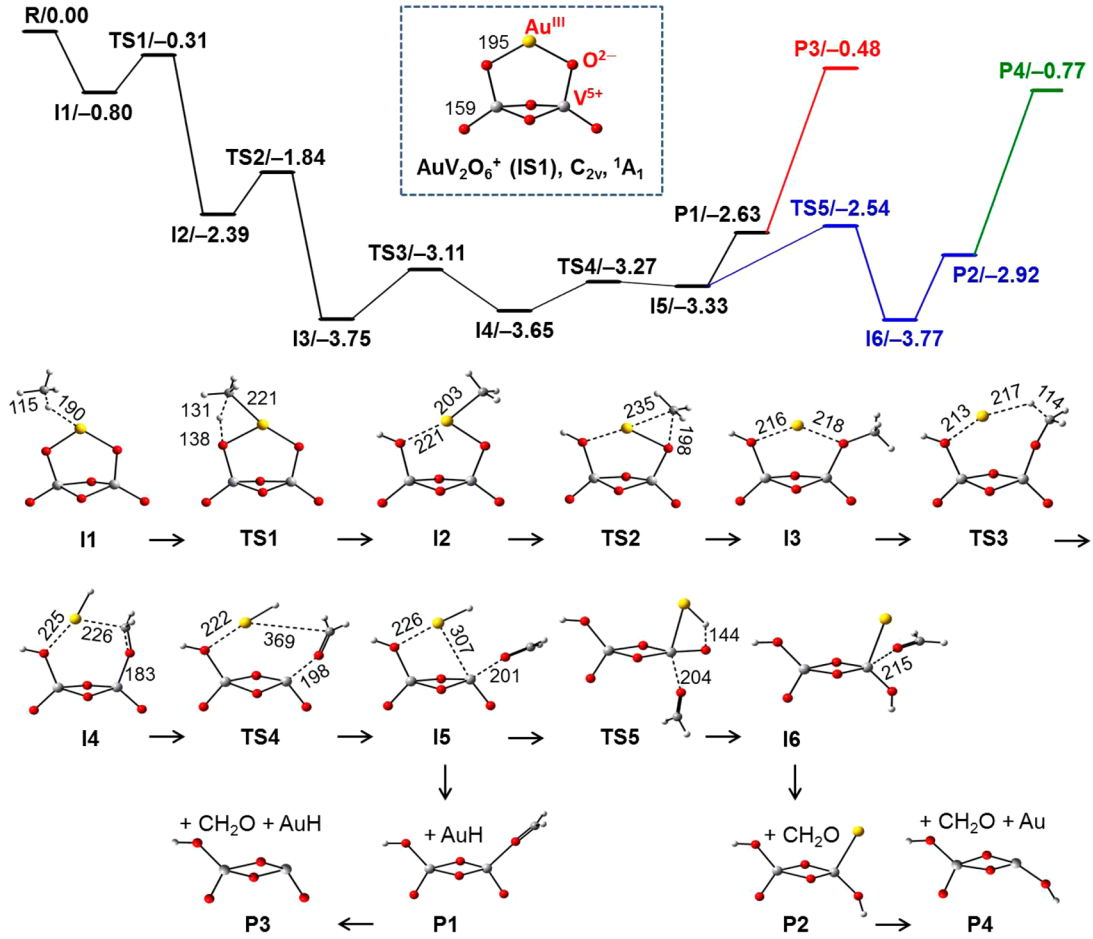

Figure 4. DFT calculated potential energy profile for reactions 1–4. The relative energies (in eV) of the reaction intermediates (I1–I6), transition states (TS1–TS5), and products (P1–P4) are with respect to the separate reactants (R). Some bond lengths (in pm) are given.

Structures and Reaction Mechanisms. The DFT calculations predicted that the most stable structure of $AuV_2O_6^+$ (labeled as IS1, see Figure 4) has the singlet electronic state and possesses two 4-fold coordinated vanadium atoms, two terminally bonded oxygen atoms, four bridging oxygen atoms, and one bridging gold atom. The gold oxidation state in IS1 is +III according to the general rules for the determination of the formal oxidation states[34] (note that six oxygen atoms carry total oxidation state of −XII, two vanadium atoms have total oxidation state of +X, and the cluster has a net positive charge).

The DFT calculations also predicted a few low-lying isomers of $AuV_2O_6^+$ with O−O and Au^I species (see IS2–IS4 in Figure S8). It turns out that these isomers are responsible for (1) the generations of $AuV_2O_4^+$ ($AuV_2O_6^+ + Ar \rightarrow AuV_2O_4^+ + O_2 + Ar$) and Au^+ in the CID experiments (Figures 3a and 3b) with low E_c values (<2.16 eV), (2) the formation of the simple addition product $AuV_2O_6CH_4^+$ in reactivity experiments (Figure 1), and (3) the dissociation of $AuV_2O_6CH_4^+$ into $AuV_2O_6^+$ and CH_4 in the PID experiments (Figure 3c). In contrast, the most stable isomer (IS1) with Au^{III} is responsible for (1) the sharp increase of Au^+ signal at E_c = 2.25–2.34 eV (Figure 3b) and (2) the reactions 1–4 to transform methane. The main text below focuses on the remarkable reactivity of the Au^{III} isomer and a detailed discussion on the Au^I isomers is given in the Supporting Information.

The DFT calculated reaction mechanism for $AuV_2O_6^+$ (IS1) + CH_4 is shown in Figure 4. When IS1 meets CH_4, the CH_4 molecule can be trapped by the Au^{III} site with a binding energy of 0.80 eV. In this process, the CH_4 is preactivated, as can be seen from the elongation of the C−H bond from 109 pm in free CH_4 to 115 pm in the encounter complex I1. It should be mentioned that methane adsorption on O atoms was also tested (Figure S10) and it turned out that the Au^{III} atom is the most favorable adsorption site. After the adsorption of methane on the Au^{III} site, the reaction proceeds with C−H bond cleavage (I1 → I2) by the Au^{III} cation in collaboration with the adjacent oxygen anion, resulting in the formations of Au−C and O−H bonds. The barrier of the above process is sufficiently low since the transition state (TS1) lies below the reactants (ΔH_0 = −0.31 eV). After the formation of I2, the methyl group can transfer from Au atom to the "oxide support" to make a chemical bond with an O atom (I2 → I3) and this step releases additional energy (1.36 eV). The reaction intermediate I3 has enough energy to transfer the H atom from the methyl group to the Au atom (I3 → I4), resulting in the formations of AuH and CH_2O moieties. Note that in I3, the CH_3 and OH groups are quite far apart; hence CH_3OH, a usual product in reactions of CH_4 with metal oxides,[35] was not produced in the experiment (Figure 1).

After a structural rearrangement (I4 → I5), the AuH unit can be easily desorbed to form P1 (reaction 1). The formation of P1 is highly exothermic, so the product ion $V_2O_6CH_3^+$ can have

DOI: 10.1021/jacs.6b03940
J. Am. Chem. Soc. 2016, 138, 9437–9443

enough internal energy to evaporate CH_2O to generate $V_2O_5H^+$ ion and the corresponding neutral species (P3, reaction 3). This reaction pathway is consistent with the result of additional reactivity experiments under different cooling gas pressures (Figure S5). Such experiments indicated that the relative intensity of $V_2O_5H^+$ was higher when the cooling gas pressure was lower. This is because the cluster ions that were less thermalized (lower cooling gas pressure) possessed higher internal energies for product fragmentation ($V_2O_6CH_3^+ \rightarrow V_2O_5H^+ + CH_2O$).

In addition to the reaction channels (1) and (3), there are competing reaction channels (2) and (4). From I5, one additional hydrogen atom transfer from the Au atom to an O atom can lead to the formation of a more stable intermediate I6 with an Au−V chemical bond. The CH_2O molecule can then be desorbed easily (I6 → P2, reaction 2). The resulting $AuV_2O_6H_2^+$ can have enough internal energy to lose the Au atom (P4, reaction 4). It is noteworthy that the energy of P1 is only slightly lower than that of TS5 (−2.63 eV versus −2.54 eV) in terms of the ΔH_0 values. However, when the entropy contribution ($-T\Delta S$) to the free energy is taken into account, the free energy of TS5 (−2.25 eV) is higher than that of P1 (−2.72 eV) significantly (0.47 eV). Therefore, the summed ion signal of $V_2O_6CH_3^+$ and $V_2O_5H^+$ can be higher than that of $AuV_2O_5H_2^+$ and $V_2O_5H_2^+$, as can be seen from Figure 1. Moreover, the formations of P1 and P2 are highly exothermic (Figure 4) and the energies of TS1−TS5 are well below that of the separate reactants (IS1 + CH_4), which means that the reaction intermediates I1−I6 all have short lifetimes[36] and have little chances to be stabilized as methane adsorption species $AuV_2O_6CH_4^+$. As a result, the $AuV_2O_6^+$ cluster isomer with the Au^{III} cation is solely responsible for methane transformation (reactions 1−4) while the methane adsorption is attributed to other low-lying isomers generated in experiments (see Supporting Information for discussion on formation of $AuV_2O_6CH_4^+$).

To further support the above assertion, the rates of traversing transition states from intermediates and the dissociation rates (k_d) of methane desorption from encounter complexes were estimated by employing the RRKM based theories.[30,31] The rates of the C−H bond activation (I1 → TS1 → I2) and the CH_4 desorption [I1 → $AuV_2O_6^+$ (IS1) + CH_4] were determined to be 1.2×10^8 s^{-1} and 4.1×10^8 s^{-1}, respectively, which are 2 orders of magnitude larger than the collision rate that a cluster experiences with the buffer gas in the ion trap reactor (about 3×10^6 s^{-1}). This indicates that I1 has a short lifetime and has a little chance to be stabilized. It is noteworthy that the larger rate of k_d than that of I1 → TS1 → I2 can be ascribed to the overestimated barrier height of TS1. When the barrier height of TS1 is reduced by 0.1 eV, the rate for I1 → TS1 → I2 would be changed to 7.9×10^8 s^{-1}, which is consistent with the observed reaction efficiency of 80% for methane transformation. This may indicate that the accuracy of the TPSS functional for the reaction barrier calculations is not better than ±0.1 eV.

Methane activation and transformation by gold-doped oxide cluster $AuNbO_3^+$ with Au^I cation and $O^{\bullet-}$ radical anion were previously studied.[12b,g] The activation of the first C−H bond of methane by $AuNbO_3^+$ proceeds with the hydrogen atom transfer to the radical center $O^{\bullet-}$ while the Au^I atom can be considered as a spectator in this process. In contrast, the reactive $AuV_2O_6^+$ with Au^{III} is a closed-shell species without the $O^{\bullet-}$ radical, so the activation of the first C−H bond of methane is mediated by the Au^{III} cation with strong Lewis acid property. In addition, the oxygen anion O^{2-} bonded with Au^{III} can be considered as Lewis base that accepts the H atom during the C−H bond cleavage (I1 → I2 in Figure 4). As a result, the C−H activation by $AuV_2O_6^+$ (IS1) follows a mechanism of cooperative effect of Lewis acid−base pairs proposed for methane activation in many condensed-phase systems including $M^{II}-O^{2-}$ (M = Pt, Pd, Mg) and $M^{III}-O^{2-}$ (M = Sc, Y, Ln, Al).[37] However, such a mechanism has been scarcely reported for methane activation by gas-phase clusters previously.[10,38] Note that the diatomic CuO^+ can activate CH_4 with the similar mechanism.[33] This study clearly demonstrates that only particular Lewis pairs $M^{n+}-O^{2-}$ can activate methane under mild conditions. On the $AuV_2O_6^+$ cluster ions, only $Au^{III}-O^{2-}$ is reactive enough to transform methane while Au^I-O^{2-} only leads to methane adsorption (see Supporting Information), which indicates that the stronger Lewis acid Au^{III} is superior to the weaker Lewis acid Au^I in terms of transformation of methane, the most stable alkane molecule.

4. CONCLUSION

The Au^{III} cation has been successfully prepared onto an early transition metal oxide cluster, and the resulting system $AuV_2O_6^+$ has remarkable reactivity in methane activation and transformation under mild conditions. Combined with the structural characterizations and quantum chemistry calculations, it is revealed that the Au^{III} species with strong Lewis acid property is the active adsorption site and facilitates the C−H bond cleavage in collaboration with the adjacent O^{2-} anion through the mechanism of cooperative Lewis acid−base pairs. Further transformation of the activated methane into formaldehyde has been identified. This study enriches the Au^{III} chemistry at a strictly molecular level and provides a fundamental basis to transform methane under mild conditions.

■ ASSOCIATED CONTENT

Supporting Information

The Supporting Information is available free of charge on the ACS Publications website at DOI: 10.1021/jacs.6b03940.

Figures and tables giving additional experimental and computational results; discussion on the cluster isomers with Au^I species; and assignments of oxidation states. (PDF)

■ AUTHOR INFORMATION

Corresponding Authors

*chemzyx@iccas.ac.cn

*shengguihe@iccas.ac.cn

Notes

The authors declare no competing financial interest.

■ ACKNOWLEDGMENTS

This work was supported by the National Natural Science Foundation of China (Nos. 21325314, 21273247, 21573247, 91545122), the Major Research Plan of China (No. 2013CB834603), and the Strategic Priority Research Program of the Chinese Academy of Sciences (XDA09030101).

■ REFERENCES

(1) (a) Haruta, M. *Catal. Today* **1997**, *36*, 153. (b) Guzman, J.; Gates, B. C. *Angew. Chem., Int. Ed.* **2003**, *42*, 690. (c) Guzman, J.; Carrettin, S.; Fierro-Gonzalez, J. C.; Hao, Y.-L.; Gates, B. C.; Corma,

DOI: 10.1021/jacs.6b03940
J. Am. Chem. Soc. 2016, 138, 9437−9443

A. *Angew. Chem., Int. Ed.* **2005**, *44*, 4778. (d) Hashmi, A. S. K.; Hutchings, G. J. *Angew. Chem., Int. Ed.* **2006**, *45*, 7896. (e) Corma, A.; Garcia, H. *Chem. Soc. Rev.* **2008**, *37*, 2096. (f) García-Mota, M.; Cabello, N.; Maseras, F.; Echavarren, A. M.; Pérez-Ramírez, J.; Lopez, N. *ChemPhysChem* **2008**, *9*, 1624. (g) Boorman, T. C.; Larrosa, I. *Chem. Soc. Rev.* **2011**, *40*, 1910. (h) Xie, J.; Pan, C.-D.; Abdukader, A.; Zhu, C.-J. *Chem. Soc. Rev.* **2014**, *43*, 5245.

(2) (a) Valden, M.; Lai, X.; Goodman, D. W. *Science* **1998**, *281*, 1647. (b) Fu, Q.; Saltsburg, H.; Flytzani-Stephanopoulos, M. *Science* **2003**, *301*, 935. (c) Chen, M.-S.; Cai, Y.; Yan, Z.; Goodman, D. W. *J. Am. Chem. Soc.* **2006**, *128*, 6341. (d) Lopez-Acevedo, O.; Kacprzak, K. A.; Akola, J.; Häkkinen, H. *Nat. Chem.* **2010**, *2*, 329. (e) Oliver-Meseguer, J.; Cabrero-Antonino, J. R.; Domínguez, I.; Leyva-Pérez, A.; Corma, A. *Science* **2012**, *338*, 1452.

(3) (a) Bond, G. C.; Thompson, D. T. *Gold Bull.* **2000**, *33*, 41. (b) Guzman, J.; Gates, B. C. *J. Am. Chem. Soc.* **2004**, *126*, 2672. (c) Chen, M.-S.; Goodman, D. W. *Catal. Today* **2006**, *111*, 22. (d) Hutchings, G. J.; Hall, M. S.; Carley, A. F.; Landon, P.; Solsona, B. E.; Kiely, C. J.; Herzing, A.; Makkee, M.; Moulijn, J. A.; Overweg, A.; Fierro-Gonzalez, J. C.; Guzman, J.; Gates, B. C. *J. Catal.* **2006**, *242*, 71. (e) Coquet, R.; Howard, K. L.; Willock, D. J. *Chem. Soc. Rev.* **2008**, *37*, 2046.

(4) (a) Bratsch, S. G. *J. Phys. Chem. Ref. Data* **1989**, *18*, 1. (b) De Vos, D. E.; Sels, B. E. *Angew. Chem., Int. Ed.* **2005**, *44*, 30. (c) Fürstner, A.; Davies, P. W. *Angew. Chem., Int. Ed.* **2007**, *46*, 3410. (d) Gorin, D. J.; Toste, F. D. *Nature* **2007**, *446*, 395.

(5) (a) Zhang, X.; Shi, H.; Xu, B.-Q. *Angew. Chem., Int. Ed.* **2005**, *44*, 7132. (b) Fierro-Gonzalez, J. C.; Bhirud, V. A.; Gates, B. C. *Chem. Commun.* **2005**, 5275. (c) Comas-Vives, A.; González-Arellano, C.; Corma, A.; Iglesias, M.; Sánchez, F.; Ujaque, G. *J. Am. Chem. Soc.* **2006**, *128*, 4756. (d) Aguilar-Guerrero, V.; Gates, B. C. *Chem. Commun.* **2007**, 3210. (e) Leyva-Pérez, A.; Corma, A. *Angew. Chem., Int. Ed.* **2012**, *51*, 614. (f) Wolf, W. J.; Winston, M. S.; Toste, F. D. *Nat. Chem.* **2013**, *6*, 159.

(6) (a) Carrettin, S.; Corma, A.; Iglesias, M.; Sánchez, F. *Appl. Catal., A* **2005**, *291*, 247. (b) Pichugina, D. A.; Kuz'menko, N. E.; Shestakov, A. F. *Gold Bull.* **2007**, *40*, 115. (c) Hopkinson, M. N.; Gee, A. D.; Gouverneur, V. *Chem. - Eur. J.* **2011**, *17*, 8248. (d) Shabbir, S.; Lee, Y.; Rhee, H. *J. Catal.* **2015**, *322*, 104. (e) Wu, C.-Y.; Horibe, T.; Jacobsen, C. B.; Toste, F. D. *Nature* **2015**, *517*, 449. (f) Kourra, C. M. B. K.; Cramer, N. *Nature* **2015**, *517*, 440.

(7) (a) Crabtree, R. H. *Chem. Rev.* **1995**, *95*, 987. (b) Fokin, A. A.; Schreiner, P. R. *Chem. Rev.* **2002**, *102*, 1551. (c) Periana, R. A.; Mironov, O.; Taube, D.; Bhalla, G.; Jones, C. *Science* **2003**, *301*, 814. (d) Guo, X.-G.; Fang, G.-Z.; Li, G.; Ma, H.; Fan, H.-J.; Yu, L.; Ma, C.; Wu, X.; Deng, D.-H.; Wei, M.-M.; Tan, D.-L.; Si, R.; Zhang, S.; Li, J.-Q.; Sun, L.-T.; Tang, Z.-C.; Pan, X.-L.; Bao, X.-H. *Science* **2014**, *344*, 616. (e) Gao, J.; Zheng, Y.; Jehng, J.-M.; Tang, Y.; Wachs, I. E.; Podkolzin, S. G. *Science* **2015**, *348*, 686.

(8) Jones, C. J.; Taube, D.; Ziatdinov, V. R.; Periana, R. A.; Nielsen, R. J.; Oxgaard, J.; Goddard, W. A., III *Angew. Chem., Int. Ed.* **2004**, *43*, 4626.

(9) (a) Pyykkö, P.; Runeberg, N. *Angew. Chem., Int. Ed.* **2002**, *41*, 2174. (b) Balaj, O. P.; Balteanu, I.; Roßteuscher, T. T. J.; Beyer, M. K.; Bondybey, V. E. *Angew. Chem., Int. Ed.* **2004**, *43*, 6519. (c) Fielicke, A.; von Helden, G.; Meijer, G.; Pedersen, D. B.; Simard, B.; Rayner, D. M. *J. Am. Chem. Soc.* **2005**, *127*, 8416. (d) Böhme, D. K.; Schwarz, H. *Angew. Chem., Int. Ed.* **2005**, *44*, 2336. (e) Johnson, G. E.; Mitrić, R.; Bonačić-Koutecký, V.; Castleman, A. W. *Chem. Phys. Lett.* **2009**, *475*, 1. (f) Castleman, A. W. *Catal. Lett.* **2011**, *141*, 1243. (g) Asmis, K. R. *Phys. Chem. Chem. Phys.* **2012**, *14*, 9270. (h) Yin, S.; Bernstein, E. R. *Int. J. Mass Spectrom.* **2012**, *321*−*322*, 49. (i) van der Linde, C.; Hemmann, S.; Höckendorf, R. F.; Balaj, O. P.; Beyer, M. K. *J. Phys. Chem. A* **2013**, *117*, 1011. (j) O'Hair, R. A. J. *Int. J. Mass Spectrom.* **2015**, *377*, 121.

(10) (a) Zhao, Y.-X.; Wu, X.-N.; Ma, J.-B.; He, S.-G.; Ding, X.-L. *Phys. Chem. Chem. Phys.* **2011**, *13*, 1925. (b) Ding, X.-L.; Wu, X.-N.; Zhao, Y.-X.; He, S.-G. *Acc. Chem. Res.* **2012**, *45*, 382. (c) Lang, S. M.; Bernhardt, T. M. *Phys. Chem. Chem. Phys.* **2012**, *14*, 9255. (d) Dietl, N.; Schlangen, M.; Schwarz, H. *Angew. Chem., Int. Ed.* **2012**, *51*, 5544.

(11) (a) Johnson, G. E.; Mitrić, R.; Nössler, M.; Tyo, E. C.; Bonačić-Koutecký, V.; Castleman, A. W. *J. Am. Chem. Soc.* **2009**, *131*, 5460. (b) Li, Z.-Y.; Zhao, Y.-X.; Wu, X.-N.; Ding, X.-L.; He, S.-G. *Chem. - Eur. J.* **2011**, *17*, 11728. (c) Tian, L.-H.; Meng, J.-H.; Wu, X.-N.; Zhao, Y.-X.; Ding, X.-L.; He, S.-G.; Ma, T.-M. *Chem. - Eur. J.* **2014**, *20*, 1167. (d) Schwarz, H. *Isr. J. Chem.* **2014**, *54*, 1413.

(12) (a) Himeno, H.; Miyajima, K.; Yasuike, T.; Mafuné, F. *J. Phys. Chem. A* **2011**, *115*, 11479. (b) Wu, X.-N.; Li, X.-N.; Ding, X.-L.; He, S.-G. *Angew. Chem., Int. Ed.* **2013**, *52*, 2444. (c) Li, Z.-Y.; Yuan, Z.; Li, X.-N.; Zhao, Y.-X.; He, S.-G. *J. Am. Chem. Soc.* **2014**, *136*, 14307. (d) Li, X.-N.; Yuan, Z.; He, S.-G. *J. Am. Chem. Soc.* **2014**, *136*, 3617. (e) Yuan, Z.; Li, X.-N.; He, S.-G. *J. Phys. Chem. Lett.* **2014**, *5*, 1585. (f) Meng, J.-H.; He, S.-G. *J. Phys. Chem. Lett.* **2014**, *5*, 3890. (g) Wang, L.-N.; Zhou, Z.-X.; Li, X.-N.; Ma, T.-M.; He, S.-G. *Chem. - Eur. J.* **2015**, *21*, 6957. (h) Li, Y.-K.; Meng, J.-H.; He, S.-G. *Int. J. Mass Spectrom.* **2015**, *381*, 10.

(13) (a) Zhao, Y.-X.; Li, Z.-Y.; Yuan, Z.; Li, X.-N.; He, S.-G. *Angew. Chem., Int. Ed.* **2014**, *53*, 9482. (b) Li, X.-N.; Yuan, Z.; Meng, J.-H.; Li, Z.-Y.; He, S.-G. *J. Phys. Chem. C* **2015**, *119*, 15414.

(14) Lopez, G. V.; Jian, T.; Li, W.-L.; Wang, L.-S. *J. Phys. Chem. A* **2014**, *118*, 5204.

(15) Yang, S.-M.; Liu, D.-M.; Liu, S.-Y. *Top. Catal.* **2008**, *47*, 101.

(16) (a) Jakubikova, E.; Rappé, A. K.; Bernstein, E. R. *J. Phys. Chem. A* **2007**, *111*, 12938. (b) Asmis, K. R.; Sauer, J. *Mass Spectrom. Rev.* **2007**, *26*, 542.

(17) (a) Justes, D. R.; Mitric, R.; Moore, N. A.; Bonacic-Koutecky, V.; Castleman, A. W. *J. Am. Chem. Soc.* **2003**, *125*, 6289. (b) Dong, F.; Heinbuch, S.; Xie, Y.; Rocca, J. J.; Bernstein, E. R.; Wang, Z.-C.; Deng, K.; He, S.-G. *J. Am. Chem. Soc.* **2008**, *130*, 1932.

(18) Yuan, Z.; Li, Z.-Y.; Zhou, Z.-X.; Liu, Q.-Y.; Zhao, Y.-X.; He, S.-G. *J. Phys. Chem. C* **2014**, *118*, 14967.

(19) Wu, X.-N.; Xu, B.; Meng, J.-H.; He, S.-G. *Int. J. Mass Spectrom.* **2012**, *310*, 57.

(20) Yuan, Z.; Zhao, Y.-X.; Li, X.-N.; He, S.-G. *Int. J. Mass Spectrom.* **2013**, *354*−*355*, 105.

(21) Kummerlöwe, G.; Beyer, M. K. *Int. J. Mass Spectrom.* **2005**, *244*, 84.

(22) (a) Xu, B.; Meng, J.-H.; He, S.-G. *J. Phys. Chem. C* **2014**, *118*, 18488. (b) Liu, Q.-Y.; Hu, L.; Li, Z.-Y.; Ning, C.-G.; Ma, J.-B.; Chen, H.; He, S.-G. *J. Chem. Phys.* **2015**, *142*, 164301.

(23) Frisch, M. J.; Trucks, G. W.; Schlegel, H. B.; Scuseria, G. E.; Robb, M. A.; Cheeseman, J. R.; Scalmani, G.; Barone, V.; Mennucci, B.; Petersson, G. A.; Nakatsuji, H.; Caricato, M.; Li, X.; Hratchian, H. P.; Izmaylov, A. F.; Bloino, J.; Zheng, G.; Sonnenberg, J. L.; Hada, M.; Ehara, M.; Toyota, K.; Fukuda, R.; Hasegawa, J.; Ishida, M.; Nakajima, T.; Honda, Y.; Kitao, O.; Nakai, H.; Vreven, T.; Montgomery, J. A., Jr.; Peralta, J. E.; Ogliaro, F.; Bearpark, M.; Heyd, J. J.; Brothers, E.; Kudin, K. N.; Staroverov, V. N.; Kobayashi, R.; Normand, J.; Raghavachari, K.; Rendell, A.; Burant, J. C.; Iyengar, S. S.; Tomasi, J.; Cossi, M.; Rega, N.; Millam, J. M.; Klene, M.; Knox, J. E.; Cross, J. B.; Bakken, V.; Adamo, C.; Jaramillo, J.; Gomperts, R.; Stratmann, R. E.; Yazyev, O.; Austin, A. J.; Cammi, R.; Pomelli, C.; Ochterski, J. W.; Martin, R. L.; Morokuma, K.; Zakrzewski, V. G.; Voth, G. A.; Salvador, P.; Dannenberg, J. J.; Dapprich, S.; Daniels, A. D.; Farkas, O.; Foresman, J. B.; Ortiz, J. V.; Cioslowski, J.; Fox, D. J. *Gaussian 09*, Revision A.1; Gaussian, Inc.: Wallingford, CT, 2009.

(24) Schäfer, A.; Huber, C.; Ahlrichs, R. *J. Chem. Phys.* **1994**, *100*, 5829.

(25) Dolg, M.; Stoll, H.; Preuss, H. *J. Chem. Phys.* **1989**, *90*, 1730.

(26) Tao, J.; Perdew, J. P.; Staroverov, V. N.; Scuseria, G. E. *Phys. Rev. Lett.* **2003**, *91*, 146401.

(27) (a) Wang, L.-N.; Li, Z.-Y.; Liu, Q.-Y.; Meng, J.-H.; He, S.-G.; Ma, T.-M. *Angew. Chem., Int. Ed.* **2015**, *54*, 11720. (b) Li, Y.-K.; Li, Z.-Y.; Zhao, Y.-X.; Liu, Q.-Y.; Meng, J.-H.; He, S.-G. *Chem. - Eur. J.* **2016**, *22*, 1825.

(28) Ding, X.-L.; Li, Z.-Y.; Meng, J.-H.; Zhao, Y.-X.; He, S.-G. *J. Chem. Phys.* **2012**, *137*, 214311.

DOI: 10.1021/jacs.6b03940
J. Am. Chem. Soc. 2016, 138, 9437−9443

(29) Berente, I.; Náray-Szabó, G. *J. Phys. Chem. A* **2006**, *110*, 772.
(30) (a) Raghavachari, K.; Trucks, G. W.; Pople, J. A.; Head-Gordon, M. *Chem. Phys. Lett.* **1989**, *157*, 479. (b) Watts, J. D.; Gauss, J.; Bartlett, R. J. *J. Chem. Phys.* **1993**, *98*, 8718. (c) Knowles, P. J.; Hampel, C.; Werner, H. J. *J. Chem. Phys.* **1993**, *99*, 5219.
(31) Steinfeld, J. I.; Francisco, J. S.; Hase, W. L. *Chemical Kinetics and Dynamics*; Prentice-Hall: Upper Saddle River, NJ, 1999; p 231.
(32) Steinfeld, J. I.; Francisco, J. S.; Hase, W. L. *Chemical Kinetics and Dynamics*; Prentice-Hall: Upper Saddle River, NJ, 1999; p 313.
(33) Beyer, T.; Swinehart, D. F. *Commun. ACM* **1973**, *16*, 379.
(34) (a) Pyykkö, P.; Runeberg, N.; Straka, M.; Dyall, K. G. *Chem. Phys. Lett.* **2000**, *328*, 415. (b) Riedel, S.; Kaupp, M. *Coord. Chem. Rev.* **2009**, *253*, 606. (c) Gong, Y.; Zhou, M.-F.; Kaupp, M.; Riedel, S. *Angew. Chem., Int. Ed.* **2009**, *48*, 7879. (d) Xiao, H.; Hu, H.-S.; Schwarz, W. H. E.; Li, J. *J. Phys. Chem. A* **2010**, *114*, 8837. (e) Wang, G.-J.; Zhou, M.-F.; Goettel, J. T.; Schrobilgen, G. J.; Su, J.; Li, J.; Schlöder, T.; Riedel, S. *Nature* **2014**, *514*, 475.
(35) (a) Chen, Y.-M.; Clemmer, D. E.; Armentrout, P. B. *J. Am. Chem. Soc.* **1994**, *116*, 7815. (b) Yoshizawa, K.; Shiota, Y.; Yamabe, T. *J. Am. Chem. Soc.* **1998**, *120*, 564. (c) Dietl, N.; van der Linde, C.; Schlangen, M.; Beyer, M. K.; Schwarz, H. *Angew. Chem., Int. Ed.* **2011**, *50*, 4966. (d) Ard, S. G.; Melko, J. J.; Ushakov, V. G.; Johnson, R.; Fournier, J. A.; Shuman, N. S.; Guo, H.; Troe, J.; Viggiano, A. A. *J. Phys. Chem. A* **2014**, *118*, 2029.
(36) Liu, Q.-Y.; He, S.-G. *Chem. J. Chin. Univ.* **2014**, *35*, 665.
(37) (a) Choudhary, V. R.; Rane, V. H. *J. Catal.* **1991**, *130*, 411. (b) Ito, T.; Tashiro, T.; Kawasaki, M.; Watanabe, T.; Toi, K.; Kobayashi, H. *J. Phys. Chem.* **1991**, *95*, 4476. (c) Burch, R.; Hayes, M. J. *J. Mol. Catal. A: Chem.* **1995**, *100*, 13. (d) Podkolzin, S. G.; Stangland, E. E.; Jones, M. E.; Peringer, E.; Lercher, J. A. *J. Am. Chem. Soc.* **2007**, *129*, 2569. (e) Wischert, R.; Copéret, C.; Delbecq, F.; Sautet, P. *Angew. Chem., Int. Ed.* **2011**, *50*, 3202. (f) Vedernikov, A. N. *Acc. Chem. Res.* **2012**, *45*, 803. (g) Guo, Z.; Liu, B.; Zhang, Q.-H.; Deng, W.-P.; Wang, Y.; Yang, Y.-H. *Chem. Soc. Rev.* **2014**, *43*, 3480.
(38) (a) Armentrout, P. B.; Beauchamp, J. L. *Acc. Chem. Res.* **1989**, *22*, 315. (b) Schröder, D.; Schwarz, H. *Proc. Natl. Acad. Sci. U. S. A.* **2008**, *105*, 18114. (c) Roach, P. J.; Woodward, W. H.; Castleman, A. W.; Reber, A. C.; Khanna, S. N. *Science* **2009**, *323*, 492. (d) Roithová, J.; Schröder, D. *Chem. Rev.* **2010**, *110*, 1170. (e) Zhao, Y.-X.; Wu, X.-N.; Wang, Z.-C.; He, S.-G.; Ding, X.-L. *Chem. Commun.* **2010**, *46*, 1736. (f) Lang, S. M.; Bernhardt, T. M.; Barnett, R. N.; Landman, U. *Angew. Chem., Int. Ed.* **2010**, *49*, 980. (g) Harding, D. J.; Kerpal, C.; Meijer, G.; Fielicke, A. *Angew. Chem., Int. Ed.* **2012**, *51*, 817. (h) Schwarz, H. *Chem. Phys. Lett.* **2015**, *629*, 91. (i) Li, H.-F.; Li, Z.-Y.; Liu, Q.-Y.; Li, X.-N.; Zhao, Y.-X.; He, S.-G. *J. Phys. Chem. Lett.* **2015**, *6*, 2287. (j) Zhao, Y.-X.; Li, X.-N.; Yuan, Z.; Liu, Q.-Y.; Shi, Q.; He, S.-G. *Chem. Sci.* **2016**, *7*, 4730. (k) Li, J.-L.; Zhou, S.-D.; Zhang, J.; Schlangen, M.; Weiske, T.; Usharani, D.; Shaik, S.; Schwarz, H. *J. Am. Chem. Soc.* **2016**, *138*, 7973.

DOI: 10.1021/jacs.6b03940
J. Am. Chem. Soc. 2016, 138, 9437−9443